Chapter 1
Functionally Fitted Continuous Finite Element Methods for Oscillatory Hamiltonian Systems

In recent decades, the numerical simulation for nonlinear oscillators has received much attention and a large number of integrators for oscillatory problems have been developed. In this chapter, based on the continuous finite element approach, we propose and analyse new energy-preserving functionally-fitted, in particular, trigonometrically-fitted methods of an arbitrarily high order for solving oscillatory nonlinear Hamiltonian systems with a fixed frequency. In order to implement these new methods in an accessable and efficient style, they are formulated as a class of continuous-stage Runge–Kutta methods. The numerical results demonstrate the remarkable accuracy and efficiency of the new methods compared with the existing high-order energy-preserving methods in the literature.

1.1 Introduction

It is known that an important area of numerical analysis and scientific computing is geometric numerical integration for differential equations. In this chapter, we consider nonlinear Hamiltonian systems:

$$\dot{y}(t) = f(y(t)) = J^{-1}\nabla H(y(t)), \quad y(t_0) = y_0 \in \mathbb{R}^d, \tag{1.1}$$

where $y \in \mathbb{R}^d$, $d = 2d_1$, $f : \mathbb{R}^d \to \mathbb{R}^d$, $H : \mathbb{R}^d \to \mathbb{R}$ are sufficiently smooth functions and

$$J = \begin{pmatrix} O_{d_1\times d_1} & I_{d_1\times d_1} \\ -I_{d_1\times d_1} & O_{d_1\times d_1} \end{pmatrix}$$

is the canonical symplectic matrix. It is well known that the flow of (1.1) preserves the symplectic form $\mathrm{d}y \wedge J\mathrm{d}y$ and the Hamiltonian or energy $H(y(t))$. In the spirit of geometric numerical integration, it is a natural idea to design schemes that preserve

X. Wu and B. Wang, *Recent Developments in Structure-Preserving Algorithms for Oscillatory Differential Equations*, https://doi.org/10.1007/978-981-10-9004-2_1

both the symplecticity of the flow and the energy. Unfortunately, however, a numerical scheme cannot achieve this goal unless it generates the exact solution (see, e.g. [23], p. 379). Hence, researchers face a choice between preserving symplecticity or preserving energy, and many of them have given more weight to the former in the last decades, and readers are referred to [23] and references therein. Despite insufficient work in the literature on energy-preserving (EP) methods (see, e.g. [1, 4, 6, 10, 11, 17, 19, 21, 29, 38]), EP methods compared with symplectic methods have better nonlinear stability properties, are easier to adapt the time step for, and are more suitable for the integration of chaotic systems (see, e.g. [12, 20, 35, 36]).

On the other hand, in scientific computing and modelling, the design and analysis of methods for periodic or oscillatory systems has been considered by many authors (see, e.g. [2, 18, 22, 34, 42, 46]). Generally, these methods utilize a priori information of special problems and they are more efficient than general-purpose methods. A popular approach to constructing methods suitable for oscillatory problems is using the functionally-fitted (FF) condition, namely, deriving a suitable method by requiring it to integrate members of a given finite-dimensional function space X exactly. If X incorporates trigonometrical or exponential functions, the corresponding methods are also called trigonometrically-fitted (TF) or exponentially-fitted (EF) methods (see, e.g. [15, 27, 32, 37]).

Therefore, combining the ideas of the EF/TF and structure-preserving methods is a promising approach to developing numerical methods which allow long-term computation of solutions to oscillatory Hamiltonian systems (1.1). Just as the research of symplectic and EP methods, EF/TF symplectic methods have been studied extensively by many authors (see, e.g. [7–9, 16, 39, 40, 43]). By contrast, as far as we know, only a few papers paid attention to the EF/TFEP methods (see, e.g. [30, 31, 41]). Usually the existing EF/TFEP methods are derived in the context of continuous-stage Runge–Kutta (RK) methods. The coefficients in these methods are determined by a system of equations resulting from EF/TF, EP and symmetry conditions. As mentioned at the end of [30], it is not easy to find such a system with a unique solution when deriving high-order methods. Furthermore, how to verify the algebraic order of such methods falls into question. A common way is to check the order conditions related to rooted trees. Again, this is inconvenient in the high-order setting since the number of trees increases extremely fast as the order grows. In this chapter, we will construct FFEP methods based on the continuous finite element method, which is inherently energy preserving (see, e.g. [1, 17, 38]). Intuitively, we expect to increase the order of the method through enlarging the finite element space. By adding trigonometrical functions to the space, the corresponding method is naturally trigonometrically fitted. Thus, we are hopeful of constructing FFEP methods, in particular TFEP methods, of arbitrarily high orders.

This chapter is organized as follows. In Sect. 1.2, we construct functionally fitted continuous finite element (FFCFE) methods and present their most important geometric properties. In Sect. 1.3, we interpret them as continuous-stage Runge–Kutta methods and analyse the algebraic order. We then discuss implementation details of these new methods in Sect. 1.4. Numerical results are shown in Sect. 1.5,

including the comparison between our new TFEP methods and other prominent structure-preserving methods in the literature. The last section is concerned with the conclusion and discussion.

1.2 Functionally-Fitted Continuous Finite Element Methods for Hamiltonian Systems

Throughout this chapter, we consider the approximation of the solution of the IVP (1.1) on the time interval $I = [t_0, T]$. Let S be a linear space of continuous functions $y(t)$ on the interval I. Let $\{\varphi_i\}_{i=0}^{r-1}$ be a family of sufficiently smooth and linearly independent real-valued functions on I, and let Y be the subspace spanned by $\{\varphi_i\}_{i=0}^{r-1}$:

$$Y = \left\{ w : w(t) = \sum_{i=0}^{r-1} W_i \varphi_i(t),\ W_i \in \mathbb{R}^d \right\}.$$

We assume that the interval $I = [t_0, T]$ is equally partitioned into $t_0 < t_1 < \ldots < t_N = T$, with $t_n = t_0 + nh$ for $n = 0, 1, \ldots, N$. A function w on I is called a *piecewise Y-type* function if for any $0 \le n \le N-1$, there exists a function $g \in Y$, such that

$$w|_{(t_n, t_{n+1})} = g|_{(t_n, t_{n+1})}.$$

It is convenient to introduce the transformation $t = t_0 + \tau h$ for $\tau \in [0, 1]$ in the following analysis. Accordingly, we denote

$$Y_h(t_0) = \{v \text{ on } [0, 1] : v(\tau) = w(t_0 + \tau h),\ w \in Y\}.$$

Hence,

$$Y_h(t_0) = \text{span}\,\{\tilde{\varphi}_0, \ldots, \tilde{\varphi}_{r-1}\},$$

where $\tilde{\varphi}_i(\tau) = \varphi_i(t_0 + \tau h)$ for $i = 0, 1, \ldots, r-1$. In what follows, lowercase Greek letters such as τ, σ, α always indicate variables on the interval [0,1] unless confusions arise.

Given two integrable functions (scalar-valued or vector-valued) w_1 and w_2 on $[0, 1]$, the inner product $\langle \cdot, \cdot \rangle$ is defined by

$$\langle w_1, w_2 \rangle = \langle w_1(\tau), w_2(\tau) \rangle_\tau = \int_0^1 w_1(\tau) \cdot w_2(\tau) d\tau,$$

where $\cdot$ is the entrywise multiplication operation if w_1, w_2 are both vector-valued functions of the same length.

Given two finite-dimensional function spaces X and Y whose members are $\mathbb{R}^d$-valued, the continuous finite element method for (1.1) is described as follows.

Find a continuous piecewise X-type function $U(t)$ on I with $U(t_0) = y_0$, such that for any piecewise function Y-type function $v(t)$,

$$\int_I v(t) \cdot (U'(t) - f(U(t)))dt = 0, \tag{1.2}$$

where $U(t) \approx y(t)$ on I and $y(t)$ solves (1.1). The term 'continuous finite element'(CFE) comes from the continuity of the finite element solution $U(t)$. Since (1.2) deals with an initial value problem, we only need to consider it on $[t_0, t_0 + h]$.

Find $u \in X_h(t_0)$ with $u(0) = y_0$, such that

$$\langle v, u' \rangle = h\langle v, f \circ u \rangle, \tag{1.3}$$

for any $v \in Y_h(t_0)$, where

$$u(\tau) = U(t_0 + \tau h) \approx y(t_0 + \tau h)$$

for $\tau \in [0, 1]$. Since $U(t)$ is continuous, $y_1 = u(1)$ is the initial value of the local problem on the next interval $[t_1, t_2]$. Thus, we can solve the global variational problem (1.2) on I step by step.

In the special case of

$$X = \text{span}\left\{1, t, \ldots, t^r\right\}, \quad Y = \text{span}\left\{1, t, \ldots, t^{r-1}\right\},$$

Equation (1.2) reduces to the classical continuous finite element method (see, e.g. [1, 25]) denoted by CFEr in this chapter. For the purpose of deriving functionally-fitted methods, we generalise X and Y a little:

$$Y = \text{span}\left\{\varphi_0(t), \ldots, \varphi_{r-1}(t)\right\}, \quad X = \text{span}\left\{1, \int_{t_0}^t \varphi_0(s)ds, \ldots, \int_{t_0}^t \varphi_{r-1}(s)ds\right\}. \tag{1.4}$$

Then it is sufficient to give X or Y since they can be determined by each other. Furthermore, Y is assumed to be invariant under translation and reflection, namely,

$$\begin{cases} v(t) \in Y \Rightarrow v(t + c) \in Y \text{ for any } c \in \mathbb{R}, \\ v(t) \in Y \Rightarrow v(-t) \in Y. \end{cases} \tag{1.5}$$

Clearly, $Y_h(t_0)$ and $X_h(t_0)$ are irrelevant to t_0 provided (1.5) holds. For convenience, we simplify $Y_h(t_0)$ and $X_h(t_0)$ by Y_h and X_h, respectively. In the remainder of this chapter, we denote the CFE method (1.2) or (1.3) based on the general function spaces (1.4) satisfying the condition (1.5) by FFCFEr.

We note that the FFCFEr method (1.3) is defined by a variational problem, and the well-definedness of this problem has not been confirmed yet. Here we presume the existence and uniqueness of the solution to (1.3). This assumption will be proved in the next section. With this premise, we are able to present three significant properties of the FFCFEr method.

We first conclude that the FFCFEr method is functionally fitted with respect to the space X, from the definition of the variational problem (1.2).

Theorem 1.1 *The FFCFEr method (1.2) solves the IVP (1.1) whose solution is a piecewise X-type function without any error.*

Moreover, the FFCFEr method is an inherently energy-preserving method. The next theorem confirms this point.

Theorem 1.2 *The FFCFEr method (1.3) exactly preserves the Hamiltonian H: $H(y_1) = H(y_0)$.*

Proof Firstly, given a vector V, we denote its ith entry by V_i. For each function $w \in Y_h$, setting $v(\tau) = w(\tau) \cdot e_i \in Y_h$ in (1.3) leads to

$$\int_0^1 w(\tau)_i u'(\tau)_i d\tau = h \int_0^1 w(\tau)_i f(u(\tau))_i d\tau, \quad i = 1, 2, \ldots, d,$$

where e_i is the ith vector of units. Hence,

$$\begin{aligned} \int_0^1 w(\tau)^{\mathsf{T}} u'(\tau) d\tau &= \sum_{i=1}^{d} \int_0^1 w(\tau)_i u'(\tau)_i d\tau = \sum_{i=1}^{d} h \int_0^1 w(\tau)_i f(u(\tau))_i d\tau \\ &= h \int_0^1 w(\tau)^{\mathsf{T}} f(u(\tau)) d\tau. \end{aligned} \tag{1.6}$$

Since $u(\tau) \in X_h$, $u'(\tau) \in Y_h$ and $J^{-1}u'(\tau) \in Y_h$, taking $w(\tau) = J^{-1}u'(\tau)$ in (1.6), we obtain

$$\begin{aligned} H(y_1) - H(y_0) &= \int_0^1 \frac{d}{d\tau} H(u(\tau)) d\tau = \int_0^1 u'(\tau)^{\mathsf{T}} \nabla H(u(\tau)) d\tau \\ &= \int_0^1 (J^{-1}u'(\tau))^{\mathsf{T}} f(u(\tau)) d\tau = h^{-1} \int_0^1 u'(\tau)^{\mathsf{T}} J u'(\tau) d\tau = 0. \end{aligned}$$

This completes the proof. □

The FFCFEr method can also be viewed as a one-step method $\Phi_h : y_0 \to y_1 = u(1)$. It is well known that reversible methods show a better long-term behaviour than nonsymmetric ones when applied to reversible differential systems such as (1.1) (see, e.g. [23]). This fact motivates the investigation of the symmetry of the FFCFEr method. Since the spaces X and Y satisfy the invariance (1.5), which is a kind of symmetry, the FFCFEr method is expected to be symmetric.

Theorem 1.3 *The FFCFEr method (1.3) is symmetric provided (1.5) holds.*

Proof It follows from (1.5) that we have $X_h = X_{-h}$, $Y_h = Y_{-h}$. Exchanging $y_0 \leftrightarrow y_1$ and replacing h with $-h$ in (1.3) give: $u(0) = y_1$, $y_0 = u(1)$, where

$$\langle v(\tau), u'(\tau)\rangle_\tau = -h\langle v(\tau), f(u(\tau))\rangle_\tau, \quad u(\tau) \in X_{-h} = X_h,$$

for each $v(\tau) \in Y_{-h} = Y_h$. Setting $u_1(\tau) = u(1-\tau) \in X_h$ and $\tau \to 1-\tau$ leads to $u_1(0) = y_0$, $y_1 = u_1(1)$, where

$$\langle v_1(\tau), u_1'(\tau)\rangle_\tau = h\langle v_1(\tau), f(u_1(\tau))\rangle_\tau,$$

for each $v_1(\tau) = v(1-\tau) \in Y_h$. This method is exactly the same as (1.3), which means that the FFCFEr method is symmetric. □

It is well known that polynomials cannot approximate oscillatory functions satisfactorily. If the problem (1.1) has a fixed frequency ω which can be evaluated effectively in advance, then the function space containing the pair $\{\sin(\omega t), \cos(\omega t)\}$ seems to be a more promising candidate for X and Y than a polynomial space. For example, possible Y spaces for deriving the TFCFE method are

$$Y_1 = \begin{cases} \text{span}\left\{\cos(\omega t), \sin(\omega t)\right\}, r = 2, \\ \text{span}\left\{1, t, \ldots, t^{r-3}, \cos(\omega t), \sin(\omega t)\right\}, r \geq 3, \end{cases} \tag{1.7}$$

$$Y_2 = \text{span}\left\{\cos(\omega t), \sin(\omega t), \ldots, \cos(k\omega t), \sin(k\omega t)\right\}, r = 2k, \tag{1.8}$$

and

$$Y_3 = \text{span}\left\{1, t, \ldots, t^p, t\cos(\omega t), t\sin(\omega t), \ldots, t^k\cos(\omega t), t^k\sin(\omega t)\right\}. \tag{1.9}$$

Correspondingly, by equipping the FFCFE method with the space $Y = Y_1$, Y_2 or Y_3, we obtain three families of TFCFE methods. According to Theorems 1.2 and 1.3, all for them are symmetric energy-preserving methods. To exemplify this framework of the TFCFE method, in numerical experiments, we will test the TFCFE method denoted by TFCFEr and TF2CFEr based on the spaces (1.7) and (1.8). It is noted that TFCFE2 and TF2CFE2 coincide.

1.3 Interpretation as Continuous-Stage Runge–Kutta Methods and the Analysis on the Algebraic Order

An interesting connection between CFE methods and RK-type methods has been shown in several papers (see, e.g. [3, 25, 38]). Since the RK methods are dominant in the numerical integration of ODEs, it is meaningful and useful to transform the FFCFEr method into the corresponding RK-type method which has been widely and conventionally used in applications. After the transformation, the FFCFEr method can be analysed and implemented by standard techniques in ODEs conveniently. To this end, it is helpful to introduce the projection operation P_h. Given a continuous $\mathbb{R}^d$-valued function w on $[0, 1]$, its projection onto Y_h, denoted by $P_h w$, is defined by

$$\langle v, P_h w\rangle = \langle v, w\rangle, \quad \text{for any } v \in Y_h. \tag{1.10}$$

Clearly, $P_h w(\tau)$ can be uniquely expressed as a linear combination of $\{\tilde{\varphi}_i(\tau)\}_{i=0}^{r-1}$:

$$P_h w(\tau) = \sum_{i=0}^{r-1} U_i \tilde{\varphi}_i(\tau), \quad U_i \in \mathbb{R}^d.$$

Taking $v(\tau) = \tilde{\varphi}_i(\tau) e_j$ in (1.10) for $i = 0, 1, \ldots, r-1$ and $j = 1, \ldots, d$, we can observe that the coefficients U_i satisfy the equation

$$M \otimes I_{d\times d} \begin{pmatrix} U_0 \\ \vdots \\ U_{r-1} \end{pmatrix} = \begin{pmatrix} \langle \tilde{\varphi}_0, w\rangle \\ \vdots \\ \langle \tilde{\varphi}_{r-1}, w\rangle \end{pmatrix},$$

where

$$M = (\langle \tilde{\varphi}_i, \tilde{\varphi}_j\rangle)_{0\le i,j\le r-1}.$$

Since $\{\tilde{\varphi}_i\}_{i=0}^{r-1}$ are linearly independent for $h > 0$, the stiffness matrix M is nonsingular. Consequently, the projection can be explicitly expressed by

$$P_h w(\tau) = \langle P_{\tau,\sigma}, w(\sigma)\rangle_\sigma,$$

where

$$P_{\tau,\sigma} = (\tilde{\varphi}_0(\tau), \ldots, \tilde{\varphi}_{r-1}(\tau)) M^{-1} (\tilde{\varphi}_0(\sigma), \ldots, \tilde{\varphi}_{r-1}(\sigma))^{\mathsf{T}}. \tag{1.11}$$

Clearly, $P_{\tau,\sigma}$ can be calculated by a basis other than $\{\tilde{\varphi}_i\}_{i=0}^{r-1}$ since they only differ in a linear transformation. If $\{\phi_0, \ldots, \phi_{r-1}\}$ is an orthonormal basis of X_h under the inner product $\langle\cdot,\cdot\rangle$, then $P_{\tau,\sigma}$ admits a simpler expression:

$$P_{\tau,\sigma} = \sum_{i=0}^{r-1} \phi_i(\tau)\phi_i(\sigma). \tag{1.12}$$

Now, using (1.3) and the definition (1.10) of the operator P_h, we obtain that $u' = hP_h(f \circ u)$ and

$$u'(\tau) = h\langle P_{\tau,\sigma}, f(u(\sigma))\rangle_\sigma. \tag{1.13}$$

Integrating the above equation with respect to τ, we transform the FFCFEr method (1.3) into the continuous-stage RK method:

$$\begin{cases} u(\tau) = y_0 + h\displaystyle\int_0^1 A_{\tau,\sigma} f(u(\sigma))d\sigma, \\ y_1 = u(1), \end{cases} \tag{1.14}$$

where

$$A_{\tau,\sigma} = \int_0^\tau P_{\alpha,\sigma} d\alpha = \sum_{i=0}^{r-1} \int_0^\tau \phi_i(\alpha) d\alpha \phi_i(\sigma). \tag{1.15}$$

In particular,

$$\phi_i(\tau) = \hat{p}_i(\tau), \tag{1.16}$$

for the CFEr method for $i = 0, 1, \ldots, r-1$, where $\hat{p}_i(\tau)$ is the shifted Legendre polynomial of degree i on $[0, 1]$, scaled in order to be orthonormal. Hence, the CFEr method in the form (1.14) is identical to the energy-preserving collocation method of order $2r$ (see [21]) or the Hamiltonian boundary value method HBVM(∞, r) (see, e.g. [4]). For the FFCFEr method, since $P_{\tau,\sigma}$, $A_{\tau,\sigma}$ are functions of variable h and $u(\tau)$ is implicitly determined by (1.14), it is necessary to analyse their smoothness with respect to h before investigating the analytic property of the numerical solution $u(\tau)$. First of all, it can be observed from (1.11) that $P_{\tau,\sigma} = P_{\tau,\sigma}(h)$ is not defined at $h = 0$ since the matrix M is singular in this case. Fortunately, however, the following lemma shows that the singularity is removable.

Lemma 1.1 *The limit,* $\lim_{h\to 0} P_{\tau,\sigma}$ *exists. Furthermore,* $P_{\tau,\sigma}$ *can be smoothly extended to* $h = 0$ *by setting* $P_{\tau,\sigma}(0) = \lim_{h\to 0} P_{\tau,\sigma}(h)$.

Proof By expanding $\{\varphi_i(t_0 + \tau h)\}_{i=0}^{r-1}$ at t_0, we obtain that

$$(\tilde{\varphi}_0(\tau), \ldots, \tilde{\varphi}_{r-1}(\tau)) = (1, \tau h, \ldots, \frac{\tau^{r-1} h^{r-1}}{(r-1)!}) W + \mathcal{O}(h^r), \tag{1.17}$$

where

$$W = \begin{pmatrix} \varphi_0(t_0) & \varphi_1(t_0) & \cdots & \varphi_{r-1}(t_0) \\ \varphi_0^{(1)}(t_0) & \varphi_1^{(1)}(t_0) & \cdots & \varphi_{r-1}^{(1)}(t_0) \\ \vdots & \vdots & & \vdots \\ \varphi_0^{(r-1)}(t_0) & \varphi_1^{(r-1)}(t_0) & \cdots & \varphi_{r-1}^{(r-1)}(t_0) \end{pmatrix} \tag{1.18}$$

is the Wronskian of $\{\varphi_i(t)\}_{i=0}^{r-1}$ at t_0, and is nonsingular. Post-multiplying the right-hand side of (1.17) by $W^{-1} diag(1, h^{-1}, \ldots, h^{1-r}(r-1)!)$ yields another basis of X_h:

$$\{1 + \mathcal{O}(h), \tau + \mathcal{O}(h), \ldots, \tau^{r-1} + \mathcal{O}(h)\}.$$

Applying the Gram–Schmidt process (with respect to the inner product $\langle \cdot, \cdot \rangle$) to the above basis, we obtain an orthonormal basis $\left\{\phi_i(\tau) = \hat{p}_i(\tau) + \mathcal{O}(h)\right\}_{i=0}^{r-1}$. Thus, by (1.12) and defining

$$P_{\tau,\sigma}(0) = \lim_{h\to 0} \sum_{i=0}^{r-1} \phi_i(\tau)\phi_i(\sigma) = \sum_{i=0}^{r-1} \hat{p}_i(\tau)\hat{p}_i(\sigma), \tag{1.19}$$

we can extend $P_{\tau,\sigma}$ to $h = 0$. Since each $\phi_i(\tau) = \hat{p}_i(\tau) + \mathscr{O}(h)$ is smooth with respect to h, $P_{\tau,\sigma}$ is also a smooth function of h. □

From (1.16) and (1.19), it can be observed that the FFCFEr method (1.14) reduces to the CFEr method when $h \to 0$, or equivalently, the energy-preserving collocation method of order $2r$ and HBVM(∞, r) method mentioned above. Since $A_{\tau,\sigma} = \int_0^\tau P_{\alpha,\sigma} d\alpha$ is also a smooth function of h, we can assume that

$$M_k = \max_{\tau,\sigma,h\in[0,1]} \left| \frac{\partial^k A_{\tau,\sigma}}{\partial h^k} \right|, \quad k = 0, 1, \ldots. \tag{1.20}$$

Furthermore, since the right function f in (1.1) maps from $\mathbb{R}^d$ to $\mathbb{R}^d$, the nth-order derivative of f at y denoted by $f^{(n)}(y)$ is a multilinear map from $\underbrace{\mathbb{R}^d \times \ldots \times \mathbb{R}^d}_{n-fold}$ to $\mathbb{R}^d$ defined by

$$f^{(n)}(y)(z_1, \ldots, z_n) = \sum_{1\le\alpha_1,\ldots,\alpha_n\le d} \frac{\partial^n f}{\partial y_{\alpha_1} \cdots \partial y_{\alpha_n}}(y) z_1^{\alpha_1} \ldots z_n^{\alpha_n},$$

where $y = (y_1, \ldots, y_d)^\intercal$ and $z_i = (z_i^1, \ldots, z_i^d)^\intercal$ for $i = 1, \ldots, n$. With this background, we now can give the existence, uniqueness, and especially the smoothness with respect to h for the continuous finite element approximation $u(\tau)$ associated with the FFCFEr method. The proof of the following theorem is based on a fixed-point iteration which is analogous to Picard iteration.

Theorem 1.4 *Given a positive constant R, let*

$$B(y_0, R) = \left\{ y \in \mathbb{R}^d : ||y - y_0|| \le R \right\}$$

and

$$D_n = \max_{y\in B(y_0,R)} ||f^{(n)}(y)||, \quad n = 0, 1, \ldots, \tag{1.21}$$

where $||\cdot|| = ||\cdot||_\infty$ is the maximum norm for vectors in $\mathbb{R}^d$ or the corresponding induced norm for the multilinear maps $f^{(n)}(y)$, $n \ge 1$. Then the FFCFEr method (1.3) or (1.14) has a unique solution $u(\tau)$ which is smoothly dependent of h provided

$$0 \le h \le \varepsilon < \min\left\{ \frac{1}{M_0 D_1}, \frac{R}{M_0 D_0}, 1 \right\}. \tag{1.22}$$

Proof Set $u_0(\tau) \equiv y_0$. We construct a function series $\{u_n(\tau)\}_{n=0}^\infty$ defined by the relation

$$u_{n+1}(\tau) = y_0 + h \int_0^1 A_{\tau,\sigma} f(u_n(\sigma)) d\sigma, \quad n = 0, 1, \ldots. \tag{1.23}$$

Obviously, $\lim_{n\to\infty} u_n(\tau)$ is a solution to (1.14) provided $\{u_n(\tau)\}_{n=0}^{\infty}$ is uniformly convergent. Thus, we only need to prove the uniform convergence of the infinite series

$$\sum_{n=0}^{\infty}(u_{n+1}(\tau) - u_n(\tau)).$$

It follows from (1.20), (1.22), (1.23) and induction that

$$||u_n(\tau) - y_0|| \le R, \quad n = 0, 1, \ldots \tag{1.24}$$

Then by using (1.21), (1.22), (1.23), (1.24) and the inequalities

$$\begin{aligned} &||\int_0^1 w(\tau)d\tau|| \le \int_0^1 ||w(\tau)||d\tau, \quad \text{for } \mathbb{R}^d\text{-valued function } w(\tau), \\ &||f(y) - f(z)|| \le D_1||y - z||, \quad \text{for } y, z \in B(y_0, R), \end{aligned}$$

we obtain the following inequalities

$$\begin{aligned} &||u_{n+1}(\tau) - u_n(\tau)|| \le h\int_0^1 M_0 D_1||u_n(\sigma) - u_{n-1}(\sigma)||d\sigma \\ &\le \beta||u_n - u_{n-1}||_c, \quad \beta = \varepsilon M_0 D_1, \end{aligned}$$

where $||\cdot||_c$ is the maximum norm for continuous functions:

$$||w||_c = \max_{\tau\in[0,1]} ||w(\tau)||, \quad w \text{ is a continuous } \mathbb{R}^d\text{-valued function on } [0, 1].$$

Therefore, we have

$$||u_{n+1} - u_n||_c \le \beta||u_n - u_{n-1}||_c$$

and

$$||u_{n+1} - u_n||_c \le \beta^n||u_1 - y_0||_c \le \beta^n R, \quad n = 0, 1, \ldots. \tag{1.25}$$

Since $\beta < 1$, according to Weierstrass M-test, $\sum_{n=0}^{\infty}(u_{n+1}(\tau) - u_n(\tau))$ is uniformly convergent, and thus, the limit of $\{u_n(\tau)\}_{n=0}^{\infty}$ is a solution to (1.14). If $v(\tau)$ is another solution, then the difference between $u(\tau)$ and $v(\tau)$ satisfies

$$||u(\tau) - v(\tau)|| \le h\int_0^1 ||A_{\tau,\sigma}(f(u(\sigma)) - f(v(\sigma)))||d\sigma \le \beta||u - v||_c,$$

and

$$||u - v||_c \le \beta||u - v||_c.$$

This means $||u - v||_c = 0$, i.e., $u(\tau) \equiv v(\tau)$. Hence, the existence and uniqueness have been proved.

As for the smooth dependence of u on h, since every $u_n(\tau)$ is a smooth function of h, we only need to prove the sequence

$$\left\{\frac{\partial^k u_n}{\partial h^k}(\tau)\right\}_{n=0}^{\infty}$$

is uniformly convergent for $k \geq 1$. Firstly, differentiating both sides of (1.23) with respect to h yields

$$\frac{\partial u_{n+1}}{\partial h}(\tau) = \int_0^1 (A_{\tau,\sigma} + h\frac{\partial A_{\tau,\sigma}}{\partial h}) f(u_n(\sigma))d\sigma + h\int_0^1 A_{\tau,\sigma} f^{(1)}(u_n(\sigma))\frac{\partial u_n}{\partial h}(\sigma)d\sigma. \quad (1.26)$$

We then have

$$||\frac{\partial u_{n+1}}{\partial h}||_c \leq \alpha + \beta||\frac{\partial u_n}{\partial h}||_c, \quad \alpha = (M_0 + \varepsilon M_1)D_0. \quad (1.27)$$

By induction, it is easy to show that $\left\{\frac{\partial u_n}{\partial h}(\tau)\right\}_{n=0}^{\infty}$ is uniformly bounded:

$$||\frac{\partial u_n}{\partial h}||_c \leq \alpha(1 + \beta + \ldots + \beta^{n-1}) \leq \frac{\alpha}{1-\beta} = C^*, \quad n = 0, 1, \ldots. \quad (1.28)$$

Combining (1.25), (1.26) and (1.28), we obtain

$$\begin{aligned}
&||\frac{\partial u_{n+1}}{\partial h} - \frac{\partial u_n}{\partial h}||_c \\
&\leq \int_0^1 (M_0 + hM_1)||f(u_n(\sigma)) - f(u_{n-1}(\sigma))||d\sigma \\
&+ h\int_0^1 M_0 \Big(||(f^{(1)}(u_n(\sigma)) - f^{(1)}(u_{n-1}(\sigma)))\frac{\partial u_n}{\partial h}(\sigma)|| \\
&\qquad + ||f^{(1)}(u_{n-1}(\sigma))(\frac{\partial u_n}{\partial h}(\sigma) - \frac{\partial u_{n-1}}{\partial h}(\sigma))|| \Big) d\sigma \\
&\leq \gamma\beta^{n-1} + \beta||\frac{\partial u_n}{\partial h} - \frac{\partial u_{n-1}}{\partial h}||_c,
\end{aligned}$$

where

$$\gamma = (M_0 D_1 + \varepsilon M_1 D_1 + \varepsilon M_0 L_2 C^*)R,$$

and L_2 is a constant satisfying

$$||f^{(1)}(y) - f^{(1)}(z)|| \leq L_2||y - z||, \quad \text{for } y, z \in B(y_0, R).$$

Thus, again by induction, we have

$$||\frac{\partial u_{n+1}}{\partial h} - \frac{\partial u_n}{\partial h}||_c \leq n\gamma\beta^{n-1} + \beta^n C^*, \quad n = 1, 2, \ldots$$

and $\left\{\frac{\partial u_n}{\partial h}(\tau)\right\}_{n=0}^{\infty}$ is uniformly convergent. By a similar argument, one can show that other function sequence $\left\{\frac{\partial^k u_n}{\partial h^k}(\tau)\right\}_{n=0}^{\infty}$ for $k \geq 2$ are uniformly convergent as well. Therefore, $u(\tau)$ is smoothly dependent on h. The proof is complete. □

Since our analysis of the algebraic order of the FFCFEr method is mainly based on Taylor's theorem, it is meaningful to investigate the expansion of $P_{\tau,\sigma}(h)$.

Proposition 1.1 *Assume that the Taylor expansion of $P_{\tau,\sigma}(h)$ with respect to h at zero is*

$$P_{\tau,\sigma} = \sum_{n=0}^{r-1} P_{\tau,\sigma}^{[n]} h^n + \mathscr{O}(h^r). \tag{1.29}$$

Then the coefficients $P_{\tau,\sigma}^{[n]}$ satisfy

$$\langle P_{\tau,\sigma}^{[n]}, g_m(\sigma)\rangle_\sigma = \begin{cases} g_m(\tau), & n = 0, \quad m = r-1, \\ 0, & n = 1, \ldots, r-1, \quad m = r-1-n, \end{cases}$$

for any $g_m \in P_m([0,1])$, where $P_m([0,1])$ consists of polynomials of degrees $\leq m$ on $[0,1]$.

Proof It can be observed from (1.11) that

$$\langle P_{\tau,\sigma}, \varphi_i(t_0 + \sigma h)\rangle_\sigma = \varphi_i(t_0 + \tau h), \quad i = 0, 1, \ldots, r-1. \tag{1.30}$$

Meanwhile, expanding $\varphi_i(t_0 + \tau h)$ at t_0 yields

$$\varphi_i(t_0 + \tau h) = \sum_{n=0}^{r-1} \frac{\varphi_i^{(n)}(t_0)}{n!}\tau^n h^n + \mathscr{O}(h^r). \tag{1.31}$$

Then by inserting (1.29) and (1.31) into the Eq. (1.30), we obtain that

$$\langle \sum_{n=0}^{r-1} P_{\tau,\sigma}^{[n]} h^n, \sum_{m=0}^{r-1} \frac{\varphi_i^{(m)}(t_0)}{m!}\sigma^m h^m\rangle_\sigma = \sum_{k=0}^{r-1} \frac{\varphi_i^{(k)}(t_0)}{k!}\tau^k h^k + \mathscr{O}(h^r).$$

Considering the terms in h^k leads to

$$\sum_{k=0}^{r-1}\left(\sum_{m+n=k}\frac{\varphi_i^{(m)}(t_0)}{m!}\langle P_{\tau,\sigma}^{[n]},\sigma^m\rangle_\sigma-\frac{\varphi_i^{(k)}(t_0)}{k!}\tau^k\right)h^k=\mathscr{O}(h^r),$$
$$\sum_{m=0}^{k-1}\frac{\varphi_i^{(m)}(t_0)}{m!}P_{m,k-m}+\frac{\varphi_i^{(k)}(t_0)}{k!}(P_{k0}-\tau^k)=0,\quad i,\ k=0,1,\ldots,r-1,$$

and

$$W^\intercal V=0,$$

where $P_{mn}=\langle P_{\tau,\sigma}^{[n]},\sigma^m\rangle_\sigma$, W is the Wronskian (1.18), and $V=(V_{mk})_{0\le m,k\le r-1}$ is an upper triangular matrix with the entries determined by

$$V_{mk}=\begin{cases}\dfrac{1}{m!}P_{m,k-m}, & m<k,\\ \dfrac{1}{m!}(P_{m,0}-\tau^m), & m=k.\end{cases}$$

Since W is nonsingular, $V=0$,

$$P_{mn}=\begin{cases}\tau^m, & n=0,\quad m+n\le r-1,\\ 0, & n=1,2,\ldots,r-1,\quad m+n\le r-1.\end{cases}\tag{1.32}$$

Then the statement of the proposition directly follows from (1.32). □

Aside from $P_{\tau,\sigma}$, it is also crucial to analyse the expansion of the solution $u(\tau)$. For convenience, we say that an h-dependent function $w(\tau)$ is regular if it can be expanded as

$$w(\tau)=\sum_{n=0}^{r-1}w^{[n]}(\tau)h^n+\mathscr{O}(h^r),$$

where

$$w^{[n]}(\tau)=\frac{1}{n!}\frac{\partial^n w(\tau)}{\partial h^n}|_{h=0}$$

is a vector-valued function with polynomial entries of degrees $\le n$.

Lemma 1.2 *Given a regular function w and an h-independent sufficiently smooth function g, the composition (if exists) is regular. Moreover, the difference between w and its projection satisfies*

$$P_h w(\tau)-w(\tau)=\mathscr{O}(h^r).$$

Proof Assume that the expansion of $g(w(\tau))$ with respect to h at zero is

$$g(w(\tau)) = \sum_{n=0}^{r-1} p^{[n]}(\tau)h^n + \mathscr{O}(h^r).$$

Then, differentiating $g(w(\tau))$ with respect to h at zero iteratively and using

$$p^{[n]}(\tau) = \frac{1}{n!}\frac{\partial^n g(w(\tau))}{\partial h^n}|_{h=0}, \quad \text{the degree of } \frac{\partial^n w(\tau)}{\partial h^n}|_{h=0} \le n, \quad n = 0, 1, \ldots, r-1,$$

we can observe that $p^{[n]}(\tau)$ is a vector with polynomial entries of degrees $\le n$ for $n = 0, 1, \ldots, r-1$ and the first statement is confirmed.

As for the second statement, using Proposition 1.1, we have

$$\begin{aligned}
&P_h w(\tau) - w(\tau)\\
&= \langle \sum_{n=0}^{r-1} P_{\tau,\sigma}^{[n]} h^n, \sum_{k=0}^{r-1} w^{[k]}(\sigma)h^k \rangle_\sigma - \sum_{m=0}^{r-1} w^{[m]}(\tau)h^m + \mathscr{O}(h^r)\\
&= \sum_{m=0}^{r-1} (\sum_{n+k=m} \langle P_{\tau,\sigma}^{[n]}, w^{[k]}(\sigma)\rangle_\sigma - w^{[m]}(\tau))h^m + \mathscr{O}(h^r)\\
&= \sum_{m=0}^{r-1} (\langle P_{\tau,\sigma}^{[0]}, w^{[m]}(\sigma)\rangle_\sigma - w^{[m]}(\tau))h^m + \mathscr{O}(h^r) = \mathscr{O}(h^r).
\end{aligned}$$

□

Before further discussions, it may be useful to recall some standard results in the theory of ODEs. To emphasize the dependence of the solution to $y'(t) = f(y(t))$ on the initial value, we assume that $y(\cdot, \tilde{t}, \tilde{y})$ solves the IVP:

$$\frac{d}{dt}y(t, \tilde{t}, \tilde{y}) = f(y(t, \tilde{t}, \tilde{y})), \quad y(\tilde{t}, \tilde{t}, \tilde{y}) = \tilde{y}.$$

Clearly, this problem is equivalent to the following integral equation:

$$y(t, \tilde{t}, \tilde{y}) = \tilde{y} + \int_{\tilde{t}}^{t} f(y(\xi, \tilde{t}, \tilde{y}))d\xi.$$

Differentiating it with respect to $\tilde{t}$ and $\tilde{y}$ and using the uniqueness of the solution leads to

$$\frac{\partial y}{\partial \tilde{t}}(t, \tilde{t}, \tilde{y}) = -\frac{\partial y}{\partial \tilde{y}}(t, \tilde{t}, \tilde{y})f(\tilde{y}). \tag{1.33}$$

With the previous analysis results, we are in a position to give the order of FFCFEr.

Theorem 1.5 *The stage order and order of the FFCFEr method (1.3) or (1.14) are r and $2r$, respectively. That is,*

$$u(\tau) - y(t_0 + \tau h) = \mathcal{O}(h^{r+1}),$$

for $0 < \tau < 1$, *and*

$$u(1) - y(t_0 + h) = \mathcal{O}(h^{2r+1}).$$

Proof Firstly, by Theorem 1.4 and Lemma 1.1, we can expand $u(\tau)$ and $A_{\tau,\sigma}$ with respect to h at zero:

$$u(\tau) = \sum_{m=0}^{r-1} u^{[m]}(\tau)h^m + \mathcal{O}(h^r), \quad A_{\tau,\sigma} = \sum_{m=0}^{r-1} A_{\tau,\sigma}^{[m]}h^m + \mathcal{O}(h^r).$$

Then let

$$\delta = u(\sigma) - y_0 = \sum_{m=1}^{r-1} u^{[m]}(\sigma)h^m + \mathcal{O}(h^r) = \mathcal{O}(h).$$

Expanding $f(u(\sigma))$ at y_0 and inserting the above equalities into the first equation of (1.14), we obtain

$$\sum_{m=0}^{r-1} u^{[m]}(\tau)h^m = y_0 + h\int_0^1 \sum_{k=0}^{r-1} A_{\tau,\sigma}^{[k]}h^k \sum_{n=0}^{r-1} F^{(n)}(y_0)(\underbrace{\delta, \ldots, \delta}_{n-fold})d\sigma + \mathcal{O}(h^r), \tag{1.34}$$

where $F^{(n)}(y_0) = f^{(n)}(y_0)/n!$. We claim that $u(\tau)$ is regular, i.e.

$$u^{[m]}(\tau) \in P_m^d = \underbrace{P_m([0,1]) \times \ldots \times P_m([0,1])}_{d-fold}$$

for $m = 0, 1, \ldots, r-1$. This fact can be confirmed by induction. Clearly, $u^{[0]}(\tau) = y_0 \in P_0^d$. If $u^{[n]}(\tau) \in P_n^d$ for $n = 0, 1, \ldots, m$, then by comparing the coefficients of h^{m+1} on both sides of (1.34) and using (1.15) and Proposition 1.1, we obtain that

$$u^{[m+1]}(\tau) = \sum_{k+n=m} \int_0^1 A_{\tau,\sigma}^{[k]} g_n(\sigma)d\sigma = \sum_{k+n=m} \int_0^\tau \int_0^1 P_{\alpha,\sigma}^{[k]} g_n(\sigma)d\sigma d\alpha$$

$$= \int_0^\tau \int_0^1 P_{\alpha,\sigma}^{[0]} g_m(\sigma)d\sigma d\alpha = \int_0^\tau g_m(\alpha)d\alpha \in P_{m+1}^d, \quad g_n(\sigma) \in P_n^d.$$

This completes the induction. By Lemma 1.2, $f(u(\tau))$ is also regular and

$$f(u(\tau)) - P_h(f \circ u)(\tau) = \mathcal{O}(h^r). \tag{1.35}$$

Then it follows from (1.13), (1.33) and (1.35) that

$$\begin{aligned} u(\tau) - y(t_0 + \tau h) &= y(t_0 + \tau h, t_0 + \tau h, u(\tau)) - y(t_0 + \tau h, t_0, y_0) \\ &= \int_0^\tau \frac{d}{d\alpha} y(t_0 + \tau h, t_0 + \alpha h, u(\alpha)) d\alpha \\ &= \int_0^\tau (h \frac{\partial y}{\partial \tilde{t}}(t_0 + \tau h, t_0 + \alpha h, u(\alpha)) + \frac{\partial y}{\partial \tilde{y}}(t_0 + \tau h, t_0 + \alpha h, u(\alpha)) u'(\alpha)) d\alpha \\ &= -h \int_0^\tau \Phi^\tau(\alpha)(f(u(\alpha)) - P_h(f \circ u)(\alpha)) d\alpha \\ &= \mathscr{O}(h^{r+1}), \end{aligned} \tag{1.36}$$

where

$$\Phi^\tau(\alpha) = \frac{\partial y}{\partial \tilde{y}}(t_0 + \tau h, t_0 + \alpha h, u(\alpha)).$$

As for the algebraic order, setting $\tau = 1$ in (1.36) leads to

$$\begin{aligned} &u(1) - y(t_0 + h) \\ &= -h \int_0^1 \Phi^1(\alpha)(f(u(\alpha)) - P_h(f \circ u)(\alpha)) d\alpha. \end{aligned} \tag{1.37}$$

Since $\Phi^1(\alpha)$ is a matrix-valued function, we partition it as $\Phi^1(\alpha) = (\Phi_1^1(\alpha), \ldots, \Phi_d^1(\alpha))^\intercal$. Using Lemma 1.2 again leads to

$$\Phi_i^1(\alpha) = P_h \Phi_i^1(\alpha) + \mathscr{O}(h^r), \quad i = 1, 2, \ldots, d. \tag{1.38}$$

Meanwhile, setting $w(\alpha) = P_h \Phi_i(\alpha)^\intercal$ in (1.6) and using (1.13) yields

$$\int_0^1 P_h \Phi_i^1(\alpha) f(u(\alpha)) d\alpha = h^{-1} \int_0^1 P_h \Phi_i^1(\alpha) u'(\alpha) d\alpha = \int_0^1 P_h \Phi_i^1(\alpha) P_h(f \circ u)(\alpha) d\alpha, \quad i = 1, 2, \ldots, d. \tag{1.39}$$

Therefore, using (1.37)–(1.39) we have

$$\begin{aligned} &u(1) - y(t_0 + h) \\ &= -h \int_0^1 \left(\begin{pmatrix} P_h \Phi_1^1(\alpha) \\ \vdots \\ P_h \Phi_d^1(\alpha) \end{pmatrix} + \mathscr{O}(h^r) \right) (f(u(\alpha)) - P_h(f \circ u)(\alpha)) d\alpha \\ &= -h \int_0^1 \begin{pmatrix} P_h \Phi_1^1(\alpha)(f(u(\alpha)) - P_h(f \circ u)(\alpha)) \\ \vdots \\ P_h \Phi_d^1(\alpha)(f(u(\alpha)) - P_h(f \circ u)(\alpha)) \end{pmatrix} d\alpha - h \int_0^1 \mathscr{O}(h^r) \times \mathscr{O}(h^r) d\alpha = \mathscr{O}(h^{2r+1}). \end{aligned}$$

□

According to Theorem 1.5, the TF CFE methods based on the spaces (1.7)–(1.9) are of order $2r$, $4k$ and $2(k + p + 1)$, respectively.

1.4 Implementation Issues

It should be noted that (1.14) is not a practical form for applications. In this section, we will detail the implementation of the FFCFEr method. Firstly, it is necessary to introduce the generalized Lagrange interpolation functions $l_i(\tau) \in X_h$ with respect to $(r+1)$ distinct points $\{d_i\}_{i=1}^{r+1} \subseteq [0,1]$:

$$(l_1(\tau), \ldots, l_{r+1}(\tau)) = (\widetilde{\Phi}_1(\tau), \widetilde{\Phi}_2(\tau), \ldots, \widetilde{\Phi}_{r+1}(\tau))\Lambda^{-1}, \tag{1.40}$$

where $\{\Phi_i(t)\}_{i=1}^{r+1}$ is a basis of X, $\widetilde{\Phi}_i(\tau) = \Phi_i(t_0 + \tau h)$ and

$$\Lambda = \begin{pmatrix} \widetilde{\Phi}_1(d_1) & \widetilde{\Phi}_2(d_1) & \ldots & \widetilde{\Phi}_{r+1}(d_1) \\ \widetilde{\Phi}_1(d_2) & \widetilde{\Phi}_2(d_2) & \ldots & \widetilde{\Phi}_{r+1}(d_2) \\ \vdots & \vdots & & \vdots \\ \widetilde{\Phi}_1(d_{r+1}) & \widetilde{\Phi}_2(d_{r+1}) & \ldots & \widetilde{\Phi}_{r+1}(d_{r+1}) \end{pmatrix}.$$

By means of the expansions

$$\Phi_i(t_0 + d_j h) = \sum_{n=0}^{r} \frac{\Phi_i^{(n)}(t_0)}{n!} d_j^n h^n + \mathscr{O}(h^{r+1}), \quad i, j = 1, 2, \ldots, r+1,$$

we have

$$\Lambda = \begin{pmatrix} 1 & d_1 h & \ldots & \frac{d_1^r h^r}{r!} \\ 1 & d_2 h & \ldots & \frac{d_2^r h^r}{r!} \\ \vdots & \vdots & & \vdots \\ 1 & d_{r+1} h & \ldots & \frac{d_{r+1}^r h^r}{r!} \end{pmatrix} \widetilde{W} + \mathscr{O}(h^{r+1}),$$

where $\widetilde{W}$ is the Wronskian of $\{\Phi_i(t)\}_{i=1}^{r+1}$ at t_0. Since $\widetilde{W}$ is nonsingular, Λ is also nonsingular for h which is sufficiently small but not zero and the Eq. (1.40) makes sense in this case. Then $\{l_i(\tau)\}_{i=1}^{r+1}$ is a basis of X_h satisfying $l_i(d_j) = \delta_{ij}$ and $u(\tau)$ can be expressed as

$$u(\tau) = \sum_{i=1}^{r+1} u(d_i) l_i(\tau).$$

Choosing $d_i = (i-1)/r$ and denoting $y_\sigma = u(\sigma)$, (1.14) now reads

$$\begin{cases} y_\sigma = \sum_{i=1}^{r+1} y_{\frac{i-1}{r}} l_i(\sigma), \\ y_{\frac{i-1}{r}} = y_0 + h \int_0^1 A_{\frac{i-1}{r},\sigma} f(y_\sigma) d\sigma, \quad i = 2, \ldots, r+1. \end{cases} \tag{1.41}$$

When f is a polynomial and $\{\Phi_i(t)\}_{i=1}^{r+1}$ are polynomials, trigonometrical or exponential functions, the integral in (1.41) can be calculated exactly. After solving this algebraic system about variables $y_{1/r}, y_{2/r}, \ldots, y_1$ by iterations, we obtain the numerical solution $y_1 \approx y(t_0 + h)$. Therefore, although the FFCFEr method can be analysed in the form of continuous-stage RK method (1.14), it is indeed an r-stage method in practice. If the integral cannot be directly calculated, we approximate it by a high-order quadrature rule $(b_k, c_k)_{k=1}^{s}$. The corresponding fully discrete scheme for (1.41) is

$$\begin{cases} y_\sigma = \sum_{i=1}^{r+1} y_{\frac{i-1}{r}} l_i(\sigma), \\ y_{\frac{i-1}{r}} = y_0 + h \sum_{k=1}^{s} b_k A_{\frac{i-1}{r}, c_k} f(y_{c_k}), \quad i = 2, \ldots, r+1. \end{cases} \tag{1.42}$$

By an argument which is similar to that stated at the beginning of Sect. 1.3, (1.42) is equivalent to a discrete version of the FFCFEr method (1.3):

$$\begin{cases} u(0) = y_0, \\ \langle v, u' \rangle_\tau = h[v, f \circ u], \quad u(\tau) \in X_h, \text{ for all } v(\tau) \in Y_h, \\ y_1 = u(1), \end{cases}$$

where $[\cdot, \cdot]$ is the discrete inner product:

$$[w_1, w_2] = [w_1(\tau), w_2(\tau)]_\tau = \sum_{k=1}^{s} b_k w_1(c_k) \cdot w_2(c_k).$$

By the proof procedure of Theorem 1.3, one can show that the fully discrete scheme is still symmetric provided the quadrature rule is symmetric, i.e. $c_{s+1-k} = 1 - c_k$ and $b_{s+1-k} = b_k$ for $k = 1, 2, \ldots, s$.

Now it is clear that the practical form (1.41) or (1.42) is determined by the Lagrange interpolation functions $l_i(\tau)$ and the coefficient $A_{\tau,\sigma}$. For the CFEr method,

$$Y_h = \text{span}\left\{1, \tau, \ldots, \tau^{r-1}\right\}, \quad X_h = \text{span}\left\{1, \tau, \ldots, \tau^{r}\right\},$$

and all $l_i(\tau)$ for $i = 1, 2, \ldots, r+1$ are Lagrange interpolation polynomials of degrees r. The $A_{\tau,\sigma}$ for $r = 2, 3, 4$ are given by

$$A_{\tau,\sigma} = \begin{cases} (4 + 6\sigma(-1 + \tau) - 3\tau)\tau, & r = 2, \\ \tau(9 - 18\tau + 10\tau^2 + 30\sigma^2(1 - 3\tau + 2\tau^2) - 12\sigma(3 - 8\tau + 5\tau^2)), & r = 3, \\ \tau(16 - 60\tau + 80\tau^2 - 35\tau^3 + 140\sigma^3(-1 + 6\tau - 10\tau^2 + 5\tau^3) \\ \quad + 60\sigma(-2 + 10\tau - 15\tau^2 + 7\tau^3) - 30\sigma^2(-8 + 45\tau - 72\tau^2 + 35\tau^3)), & r = 4. \end{cases}$$

For the TFCFEr method,

$$Y = \text{span}\left\{1, t, \ldots, t^{r-3}, \cos(\omega t), \sin(\omega t)\right\},$$

then

$$Y_h = \text{span}\left\{1, \tau, \ldots, \tau^{r-3}, \cos(\nu\tau), \sin(\nu\tau)\right\},$$
$$X_h = \text{span}\left\{1, \tau, \ldots, \tau^{r-2}, \cos(\nu\tau), \sin(\nu\tau)\right\},$$

where $\nu = h\omega$. The corresponding $A_{\tau,\sigma}$ and $l_i(\tau)$ are more complicated than those of CFEr, but one can calculate them by the formulae (1.15) and (1.40) without any difficulty before solving the IVP numerically. Consequently, the computational cost of the TFCFEr method at each step is comparable to that of the CFEr method. Besides, when ν is small, in order to avoid unacceptable cancellation, it is recommended to calculate variable coefficients in TF methods by their Taylor expansions with respect to ν at zero.

1.5 Numerical Experiments

In this section, we carry out four numerical experiments to test the effectiveness and efficiency of the new methods TFCFEr based on the space (1.7) for $r = 2, 3, 4$ and TF2CFE4 based on the space (1.8) in the long-term computation of structure preservation. These new methods are compared with standard r-stage $2r$th-order EP CFEr methods for $r = 2, 3, 4$. Other methods such as the 2-stage 4th-order EF symplectic Gauss–Legendre collocation method (denoted by EFGL2) derived in [7] and the 2-stage 4th-order EF EP method (denoted by EFCRK2) derived in [30] are also considered. Since all of these structure-preserving methods are implicit, fixed-point iterations are needed to solve the nonlinear algebraic systems at each step. The tolerance error for the iteration solution is set to 10^{-15} in the numerical simulation.

Numerical quantities with which we are mainly concerned are the Hamiltonian error

$$EH = (EH^0, EH^1, \ldots),$$

with

$$EH^n = |H(y_n) - H(y_0)|,$$

and the solution error

$$ME = (ME^0, ME^1, \ldots),$$

with

$$ME^n = ||y_n - y(t_n)||_\infty.$$

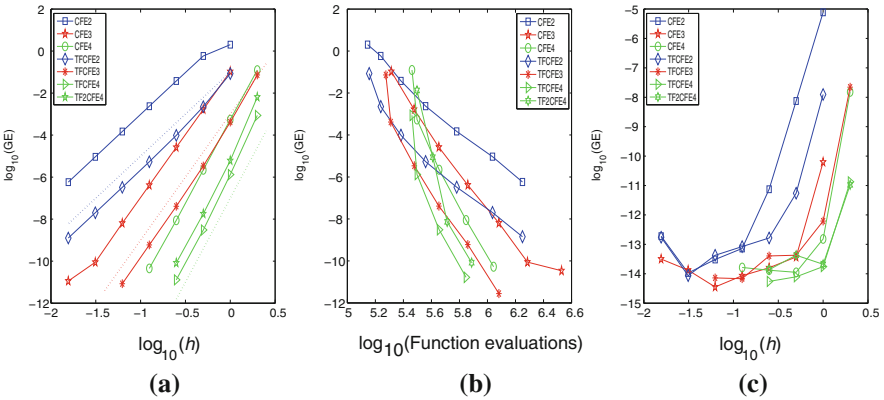

Fig. 1.1 **a** The logarithm of the maximum global error against the logarithm of the stepsize. The dashed lines have slopes four, six and eight. **b** The logarithm of the maximum global error against the logarithm of function evaluations. **c** The logarithm of the maximum global error of Hamiltonian against the logarithm of the stepsize.

Correspondingly, the maximum global errors of Hamiltonian (GEH) and the solution (GE) are defined by:

$$GEH = \max_{n\geq 0} EH^n, \quad GE = \max_{n\geq 0} ME^n,$$

respectively. Here the numerical solution at the time node t_n is denoted by y_n.

Example 1.1 Consider the Perturbed Kepler problem defined by the Hamiltonian:

$$H(p,q) = \frac{1}{2}(p_1^2 + p_2^2) - \frac{1}{(q_1^2+q_2^2)^{\frac{1}{2}}} - \frac{2\varepsilon+\varepsilon^2}{3(q_1^2+q_2^2)^{\frac{3}{2}}},$$

with the initial condition $q_1(0) = 1, q_2 = 0, p_1(0) = 0, p_2 = 1+\varepsilon$, where ε is a small parameter. The exact solution of this IVP is

$$q_1(t) = \cos((1+\varepsilon)t), \quad q_2(t) = \sin((1+\varepsilon)t), \quad p_i(t) = q_i'(t),\ i = 1, 2.$$

Taking $\omega = 1, \varepsilon = 0.001$ and $h = 1/2^i$ for $i = -1, 0, \ldots, 6$, we integrate this problem over the interval $[0, 200\pi]$ by the TF2CFE4, TFCFEr and CFEr methods for $r = 2, 3, 4$. The nonlinear integral in the r-stage method is evaluated by the $(r+1)$-point Gauss–Legendre quadrature rule. Numerical results are presented in Fig. 1.1.

From Fig. 1.1a it can be observed that TFCFEr and TF2CFE4 methods show the expected order. Under the same stepsize, the TF method is more accurate than the non-TF method of the same order. Since the double precision provides only 16 significant digits, the numerical results are polluted significantly by rounding errors

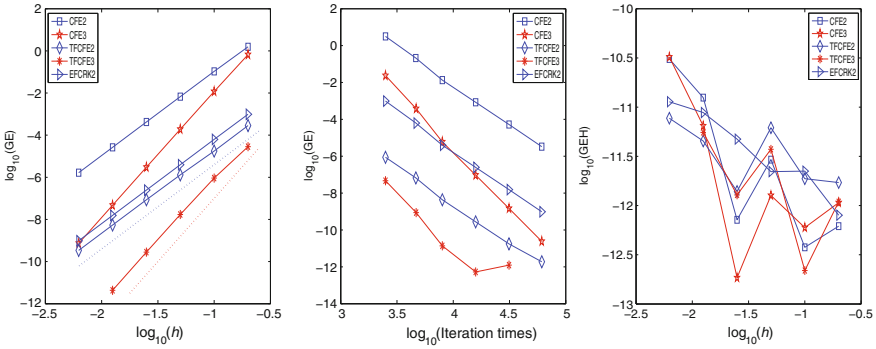

Fig. 1.2 **a** The logarithm of the maximum global error against the logarithm of the stepsize. The dashed lines have slopes four and six. **b** The logarithm of the maximum global error against the logarithm of iteration times. **c** The logarithm of the maximum global error of Hamiltonian against the logarithm of the stepsize.

when the maximum global error attains the magnitude 10^{-11}. Figure 1.1b shows that the efficiency of the TF method is higher than that of the non-TF method of the same order. Besides, high-order methods are more efficient than low-order ones when the stepsize is relatively small.

In Fig. 1.1c, one can see that all of these EP methods preserve the Hamiltonian very well. The errors in the Hamiltonian are mainly contributed by the quadrature error when the stepsize h is large and the rounding error when h is small.

Example 1.2 Consider the Duffing equation defined by the Hamiltonian:

$$H(p,q) = \frac{1}{2}p^2 + \frac{1}{2}(\omega^2 + k^2)q^2 - \frac{k^2}{2}q^4$$

with the initial value $q(0) = 0$, $p(0) = \omega$. The exact solution of this IVP is

$$q(t) = sn(\omega t; k/\omega), \quad p(t) = cn(\omega t; k/\omega)dn(\omega t; k/\omega).$$

where sn, cn and dn are Jacobi elliptic functions. Taking $k = 0.07$, $\omega = 5$ and $h = 1/5 \times 1/2^i$ for $i = 0, 1, \ldots, 5$, we integrate this problem over the interval $[0, 100]$ by TFCFE2, TFCFE3, CFE2, CFE3 and EFCRK2 methods. Since the nonlinear term f is polynomial, we can calculate the integrals involved in these methods exactly by Mathematica at the beginning of the computation. Numerical results are shown in Fig. 1.2.

In Fig. 1.2a, one can see that the TF method is more accurate than the non-TF method of the same order under the same stepsize. For both as 2-stage $4th$-order methods, TFCFE2 method is more accurate than EFCRK2 method for this problem.

Again, it can be observed from Fig. 1.2b that the efficiency of the CFEr method is lower than that of the EF/TF method of the same order. Although the nonlinear integrals are exactly calculated in theory, Fig. 1.2c shows that all of these methods only approximately preserve the Hamiltonian. It seems that the rounding error increases as $h \to 0$.

Example 1.3 Consider the Fermi–Pasta–Ulam problem studied by Hairer et al. in [22, 23], which is defined by the Hamiltonian

$$H(p,q) = \frac{1}{2}p^{\mathsf{T}}p + \frac{1}{2}q^{\mathsf{T}}Mq + U(q),$$

where

$$M = \begin{pmatrix} O_{m\times m} & O_{m\times m} \\ O_{m\times m} & \omega^2 I_{m\times m} \end{pmatrix},$$
$$U(q) = \frac{1}{4}\left((q_1 - q_{m+1})^4 + \sum_{i=1}^{m-1}(q_{i+1} - q_{m+i+1} - q_i - q_{m+i})^4 + (q_m + q_{2m})^4\right).$$

In this problem, we choose $m = 2$, $q_1(0) = 1$, $p_1(0) = 1$, $q_3(0) = 1/\omega$, $p_3(0) = 1$, and zero for the remaining initial values. Setting $\omega = 50$, $h = 1/50$ and $\omega = 100$, $h = 1/100$, we integrate this problem over the interval $[0, 100]$ by CFE2, CFE3, TFCFE2, TFCFE3 and EFCRK2 methods. The nonlinear integrals are calculated exactly by Mathematica at the beginning of the computation. We choose the numerical solution obtained by a high-order method with a sufficiently small stepsize as the 'reference solution' in the FPU problem. Numerical results are plotted in Fig. 1.3.

In Fig. 1.3a, c, one can see that the TF methods are more accurate than non-TF ones. Unlike the previous problem, the EFCRK2 method wins slightly over TFCFE2 method in this case. The Fig. 1.3b, d also show that all of these methods display promising EP property, which is especially important in the FPU problem.

Example 1.4 Consider the IVP defined by the nonlinear Schrödinger equation

$$\begin{cases} iu_t + u_{xx} + 2|u|^2 u = 0, \\ u(x,0) = \varphi(x), \end{cases} \tag{1.43}$$

where u is a complex function of x, t, and i is the imaginary unit. Taking the periodic boundary condition $u(x_0, t) = u(x_0 + L, t)$ and discretizing the spatial derivative ∂_{xx} by the pseudospectral method (see e.g. [13]), this problem is converted into a complex system of ODEs:

$$\begin{cases} i\dfrac{d}{dt}U + D^2U + 2|U|^2 \cdot U = 0, \\ U(0) = (\varphi(x_0), \varphi(x_1), \ldots, \varphi(x_{d-1}))^{\mathsf{T}}, \end{cases}$$

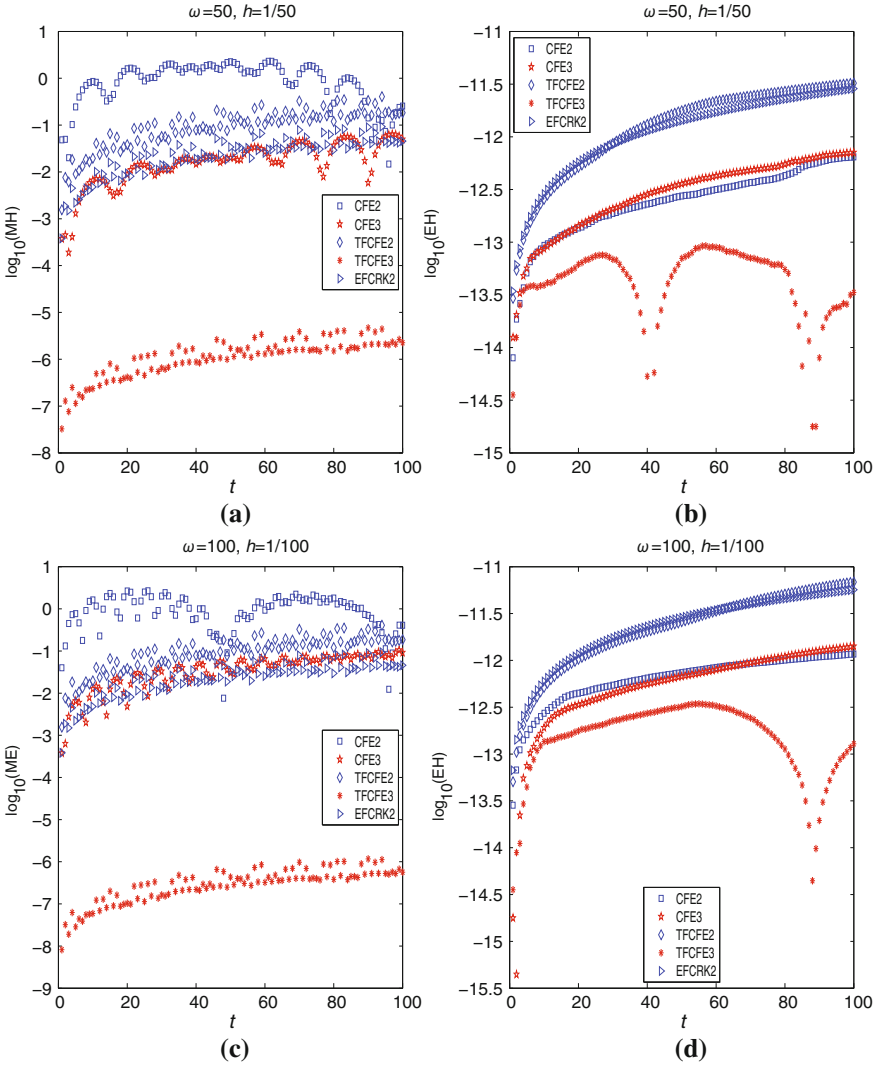

Fig. 1.3 **a**, **c** The logarithm of the solution error against time t. **b**, **d** The logarithm of the Hamiltonian error against time t.

or an equivalent Hamiltonian system:

$$\begin{cases} \dfrac{d}{dt}P = -D^2Q - 2(P^2+Q^2)\cdot Q, \\ \dfrac{d}{dt}Q = D^2P + 2(P^2+Q^2)\cdot P, \\ P(0) = real(U(0)), \quad Q(0) = imag(U(0)), \end{cases} \tag{1.44}$$

where the superscript '2' is the entrywise square multiplication operation for vectors, $x_n = x_0 + n\Delta x/d$ for $n = 0, 1, \ldots, d-1$, $U = (U_0(t), U_1(t), \ldots, U_{d-1}(t))^\intercal$, $P(t) = real(U(t))$, $Q(t) = imag(U(t))$ and $D = (D_{jk})_{0\le j,k\le d-1}$ is the pseudospectral differential matrix defined by:

$$D_{jk} = \begin{cases} \frac{\pi}{L}(-1)^{j+k}\cot(\pi\frac{x_j - x_k}{L}), & j \neq k, \\ 0, & j = k. \end{cases}$$

The Hamiltonian or the total energy of (1.44) is

$$H(P, Q) = \frac{1}{2}P^\intercal D^2 P + \frac{1}{2}Q^\intercal D^2 Q + \frac{1}{2}\sum_{i=0}^{d-1}(P_i^2 + Q_i^2)^2.$$

In [33], the author constructed a periodic bi-soliton solution of (1.43):

$$u(x,t) = \frac{\Phi}{\Psi}, \tag{1.45}$$

where

$$\begin{aligned} \Phi &= (\exp(iM^2t)M\cosh^{-1}(M(x-A)) - \exp(iN^2t)N\cosh^{-1}(N(x+A))), \\ \Psi &= (\cosh(J) - \sinh(J)(\tanh(M(x-A))\tanh(N(x+A)) \\ &\quad + \cos((M^2-N^2)t)\cosh^{-1}(M(x-A))\cosh^{-1}(N(x+A)))) \end{aligned}$$

with

$$J = \tanh^{-1}(\frac{2MN}{M^2+N^2}).$$

This solution can be viewed approximately as the superposition of two single solitons located at $x = A$ and $x = -A$ respectively. Since it decays exponentially when $x \to \infty$, we can take the periodic boundary condition for sufficiently small x_0 and large L with little loss of accuracy. Aside from the total energy, it is well known that the semi-discrete NLS (1.44) has another invariant, the total charge

$$C(P, Q) = \sum_{i=0}^{d-1}(P_i^2 + Q_i^2).$$

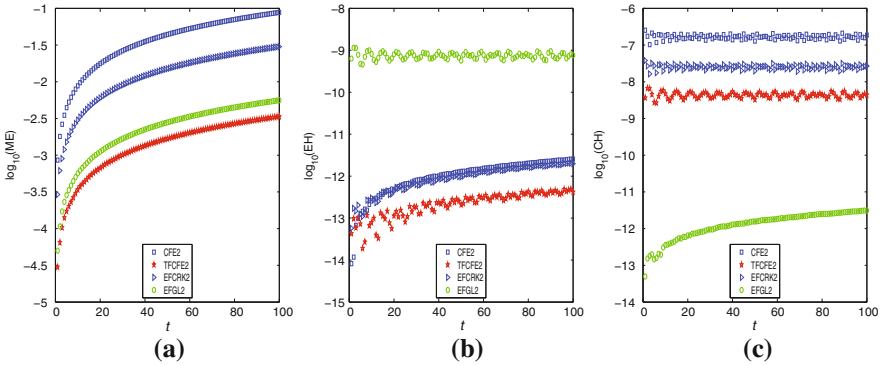

Fig. 1.4 **a** The logarithm of the solution error against time t (left). **b** The logarithm of the Hamiltonian error against time t (middle). **c** The logarithm of the charge error against time t (right).

Thus, we also calculate the error in the charge (EC):

$$EC = (EC^0, EC^1, \ldots)$$

with

$$EC^n = |C^n - C^0|, \quad C^n = C(P^n, Q^n)$$

where $P^n \approx P(t_n)$, $Q^n \approx Q(t_n)$ is the numerical solution at the time node t_n. Taking $x_0 = -50$, $L = 100$, $A = 10$, $M = 1$, $N = 2^{\frac{1}{2}}$, $d = 450$, $h = 0.2$, $\omega = 2$, we integrate the semi-discrete problem (1.44) by the TFCFE2, CFE2 and EFGL2 methods over the time interval $[0, 100]$. The nonlinear integrals are calculated exactly by Mathematica at the beginning of the computation. Numerical results are presented in Fig. 1.4.

It is noted that the exact solution (1.45) has two approximate frequency M^2 and N^2. By choosing the larger frequency $N^2 = 2$ as the fitting frequency ω, the EF/TF methods still reach higher accuracy than the general-purpose method CFE2, see Fig. 1.4a. Among three EF/TF methods, TFCFE2 is the most accurate. Figure 1.4b shows that three EP methods CFE2, TFCFE2 and EFCRK2 preserve the Hamiltonian (apart from the rounding error). Since EFGL2 is a symplectic method, it preserves the discrete charge, which is a quadratic invariant, see Fig. 1.4c. Although TFCFE2 method cannot preserve the discrete charge, its error in the charge is smaller than the charge errors of CFE2 and EFCRK2.

1.6 Conclusions and Discussions

Highly oscillatory systems constitute an important category of differential equations in applied sciences. The numerical treatment of oscillatory systems is full of challenges. Readers are referred to Hairer et al. [23], Iserles [26], Petzold et al. [14], Cohen et al. [34], Wu et al. [44, 45], and references contained therein. This chapter is mainly concerned with the establishment of high-order functionally-fitted energy-preserving methods for solving oscillatory nonlinear Hamiltonian systems. We have derived new FFCFEr methods based on the analysis of continuous finite element methods. The FFCFEr methods can be thought of as a continuous-stage Runge–Kutta methods, and hence it can be used conveniently in applications. The geometric properties and algebraic orders of the method have been analysed in detail. By equipping FFCFEr with the spaces (1.7) and (1.8), we have developed the TFEP methods denoted by TFCFEr and TF2CFEr which are suitable for solving oscillatory Hamiltonian systems with a fixed frequency ω. Evaluating the nonlinear integrals in the EP methods exactly or approximately, we have compared TFCFEr for $r = 2, 3, 4$ and TF2CFE4 with other structure-preserving methods such as EP methods CFEr for $r = 2, 3, 4$, the EP method EFCRK2 and the symplectic method EFGL2. The numerical results show that the newly derived TFEP methods exhibit definitely a high accuracy, an excellent invariant-preserving property and a prominent long-term behaviour.

In numerical experiments, we are mainly concerned with the TFCFEr methods when applied to oscillatory Hamiltonian systems. However, the FFCFEr methods, by nature, are symmetric and of order $2r$ for the general autonomous system $y'(t) = f(y(t))$. By choosing appropriate function spaces, the FFCFEr methods can be applied to solve a much wider class of dynamic systems in applications. For example, the application of the FF Runge–Kutta method to the stiff system has been shown in [32]. Consequently, we conclude that FFCFEr methods are likely to be a class of highly flexible methods with many potential applications.

In conclusion, in this chapter, from the perspective of the continuous finite element method, we have presented and analysed energy-preserving functionally fitted methods, in particular, trigonometrically fitted methods of an arbitrarily high order for solving oscillatory nonlinear Hamiltonian systems with a fixed frequency. In the next chapters, we will consider multi-frequency highly oscillatory systems.

This chapter is based on the work of Li and Wu [28].

References

1. Betsch, P., Steinmann, P.: Inherently energy conserving time finite element methods for classical mechanics. J. Comput. Phys. **160**, 88–116 (2000)
2. Bettis, D.G.: Numerical integration of products of Fourier and ordinary polynomials. Numer. Math. **14**, 424–434 (1970)

3. Bottasso, C.L.: A new look at finite elements in time : a variational interpretation of Runge-Kutta methods. Appl. Numer. Math. **25**, 355–368 (1997)
4. Brugnano, L., Iavernaro, F., Trigiante, D.: Hamiltonan boundary value methods (Energy preserving discrete line integral methods). J. Numer. Anal. Ind. Appl. Math. **5**, 13–17 (2010)
5. Brugnano, L., Iavernaro, F., Trigiante, D.: A simple framework for the derivation and analysis of effective one-step methods for ODEs. Appl. Math. Comput. **218**, 8475–8485 (2012)
6. Brugnano, L., Iavernaro, F., Trigiante, D.: Energy- and quadratic invariants-preserving integrators based upon Gauss-collocation formulae. SIAM J. Numer. Anal. **50**, 2897–2916 (2012)
7. Calvo, M., Franco, J.M., Montijano, J.I., Rández, L.: Structure preservation of exponentially fitted Runge-Kutta methods. J. Comput. Appl. Math. **218**, 421–434 (2008)
8. Calvo, M., Franco, J.M., Montijano, J.I., Rández, L.: Symmetric and symplectic exponentially fitted Runge-Kutta methods of high order. Comput. Phys. Commun. **181**, 2044–2056 (2010)
9. Calvo, M., Franco, J.M., Montijano, J.I., Rández, L.: On high order symmetric and symplectic trigonometrically fitted Runge-Kutta methods with an even number of stages. BIT Numer. Math. **50**, 3–21 (2010)
10. Celledoni, E., Mclachlan, R.I., Mclaren, D.I., Owren, B., Quispel, G.R.W., Wright, W.M.: Energy-preserving Runge-Kutta methods. ESIAM. Math. Model. Numer. Anal. **43**, 645–649 (2009)
11. Celledoni, E., Mclachlan, R.I., Owren, B., Quispel, G.R.W.: Energy-preserving integrators and the structure of B-series. Found. Comput. Math. **10**, 673–693 (2010)
12. Celledoni, E., Grimm, V., Mclachlan, R.I., Mclaren, D.I., O'Neale, D., Owren, B., Quispel, G.R.W.: Preserving energy resp. dissipation in numerical PDEs using the 'Average Vector Field' method. J. Comput. Phys. **231**, 6770–6789 (2012)
13. Chen, J.B., Qin, M.Z.: Multisymplectic fourier pseudospectral method for the nonlinear Schrödinger equation. Electron. Trans. Numer. Anal. **12**, 193–204 (2001)
14. Cohen, D., Jahnke, T., Lorenz, K., Lubich, C.: Numerical integrators for highly oscillatory Hamiltonian systems: a review. In: Mielke, A. (ed.) Analysis, Modeling and Simulation of Multiscale Problems, pp. 553–576. Springer, Berlin (2006)
15. Coleman, J.P.: P-stability and exponential-fitting methods for $y'' = f(x, y)$. IMA J. Numer. Anal. **16**, 179–199 (1996)
16. Franco, J.M.: Exponentially fitted symplectic integrators of RKN type for solving oscillatory problems. Comput. Phys. Commun. **177**, 479–492 (2007)
17. French, D.A., Schaeffer, J.W.: Continuous finite element methods which preserve energy properties for nonlinear problems. Appl. Math. Comput. **39**, 271–295 (1990)
18. Gautschi, W.: Numerical integration of ordinary differential equations based on trigonometric polynomials. Numer. Math. **3**, 381–397 (1961)
19. Gonzalez, O.: Time integration and discrete hamiltonian systems. J. Nonlinear Sci. **6**, 449–467 (1996)
20. Hairer, E.: Variable time step integration with symplectic methods. Appl. Numer. Math. **25**, 219–227 (1997)
21. Hairer, E.: Energy-preserving variant of collocation methods. J. Numer. Anal. Ind. Appl. Math. **5**, 73–84 (2010)
22. Hairer, E., Lubich, C.: Long-time energy conservation of numerical methods for oscillatory differential equations. SIAM J. Numer. Anal. **38**, 414–441 (2000)
23. Hairer, E., Lubich, C., Wanner, G.: Geometric Numerical Integration, 2nd edn. Springer, Berlin (2006)
24. Huang, N.S., Sidge, R.B., Cong, N.H.: On functionally fitted Runge-Kutta methods. BIT Numer. Math. **46**, 861–874 (2006)
25. Hulme, B.L.: One-step piecewise polynomial Galerkin methods for initial value problems. Math. Comput. **26**, 415–426 (1972)
26. Iserles, A.: On the method of Neumann series for highly oscillatory equations. BIT Numer. Math. **44**, 473–488 (2004)
27. Ixaru, L.G., Vanden Bergehe, G. (eds.): Exponential Fitting. Kluwer Academic Publishers, Dordrecht (2004)

28. Li, Y.W., Wu, X.Y.: Functionally-fitted energy-preserving methods for solving oscillatory nonlinear Hamiltonian systems. SIAM J. Numer. Anal. **54**, 2036–2059 (2016)
29. Mclachlan, R.I., Quispel, G.R.W., Robidoux, N.: Geometric integration using dicrete gradients. Philos. Trans. R. Soc. A **357**, 1021–1046 (1999)
30. Miyatake, Y.: An energy-preserving exponentially-fitted continuous stage Runge-Kutta method for Hamiltonian systems. BIT Numer. Math. **54**, 777–799 (2014)
31. Miyatake, Y.: A derivation of energy-preserving exponentially-fitted integrators for poisson systems. Comput. Phys. Commun. **187**, 156–161 (2015)
32. Ozawa, K.: A functionally fitting Runge-Kutta method with variable coefficients. Jpn. J. Ind. Appl. Math. **18**, 107–130 (2001)
33. Peregrine, D.H.: Water waves, nonlinear Schrödinger equations and their solutions. J. Austral. Math. Soc. Ser B **25**, 16–43 (1983)
34. Petzold, L.R., Jay, L.O., Jeng, Y.: Numerical solution of highly oscillatory ordinary differential equations. Acta Numer. **6**, 437–483 (1997)
35. Simos, J.C.: Assessment of energy-momentum and symplectic schemes for stiff dynamical systems. In: American Sociery for Mechanical Engineers, ASME Winter Annual meeting, New Orleans, Louisiana (1993)
36. Simos, T.E.: Does variable step size ruin a symplectic integrator? Phys. D. Nonlinear Phenom. **60**, 311–313 (1992)
37. Simos, T.E.: An exponentially-fitted Rung-Kutta method for the numerical integration of initial-value problems with periodic or oscillating solutions. Comput. Phys. Commun. **115**, 1–8 (1998)
38. Tang, W., Sun, Y.: Time finite element methods : A unified framework for the numerical discretizations of ODEs. Appl. Math. Comput. **219**, 2158–2179 (2012)
39. Vande Vyver, H.: A fourth order symplectic exponentially fitted integrator. Comput. Phys. Commun. **176**, 255–262 (2006)
40. Vanden Berghe, G., Daele, M., Vande Vyver, H.: Exponentially-fitted Runge-Kutta methods of collocation type : fixed or variable knots? J. Comput. Appl. Math. **159**, 217–239 (2003)
41. Wang, B., Wu, X.Y.: A new high precision energy-preserving integrator for system of second-order differential equations. Phys. Lett. A **376**, 1185–1190 (2012)
42. Wang, B., Iserles, A., Wu, X.Y.: Arbitrary order trigonometric fourier collocation methods for multi-frequency oscillatory systems. Found. Comput. Math. **16**, 151–181 (2016)
43. Wu, X.Y., Wang, B., Xia, J.: Explicit symplectic multidimensional exponential fitting modified Runge-Kutta-Nyström methods. BIT Numer. Math. **52**, 773–791 (2012)
44. Wu, X.Y., You, X., Wang, B.: Structure-Preserving Algorithms for Oscillatory Differential Equations. Springer, Berlin (2013)
45. Wu, X.Y., Liu, K., Shi, W.: Structure-Preserving Algorithms for Oscillatory Differential Equations II. Springer, Berlin (2015)
46. Yang, H., Wu, X.Y., You, X., Fang, Y.: Extended RKN-type methods for numerical integration of perturbed oscillators. Comput. Phys. Commun. **180**, 1777–1794 (2009)